

The Rotational Spectrum and Enharmonic Force Field of Chlorine Dioxide, OC1O

Holger S. P. Müller,^{*,1} G. Ole Sørensen,[†] Manfred Birk,^{*,2} and Randy R. Friedl^{*}

^{}Jet Propulsion Laboratory, California **Institute** of Technology, Mail Stop 183-301, 4800 Oak
Grove Drive, Pasadena, California 91109-8099; and*

*[†]Chemical Laboratory, H. C. Ørsted Institute, University of Copenhagen, Universitetsparken 5,
DK-2100 Copenhagen Ø, Denmark*

Received

¹Present address: I. Physikalisches Institut, Universität zu Köln, Zùlpicher Str. 77, D-50937 Köln,
Germany. E-mail: hspm@spec.nasa.gov.

²Present address: Institut für Optoelektronik, DLR, D-82234 Oberpfaffenhofen, Germany.

No. of pages: 35

No. of Tables: 16

no figures

Proposed running head: Rotational spectrum and force field of OC1O.

Send proofs to

Holger S. P. Müller

z. Hd. Prof. G. Winnewisser

I. Physikalisches Institut

Universität zu Köln

Zülpicher Str. 77

D-50937 Köln

Germany

E-mail: hspm@spec.nasa.gov.

Fax: 011-49-221-470-5162

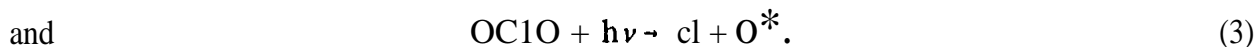
The rotational spectra of 0^{35}C10 and $0^{3'}\text{C10}$ in their (000), (100), (010), (001), and (020) states have been reinvestigated in selected regions between 130 and 526 GHz. About 800 newly measured lines spanning the quantum numbers $2 \leq N \leq 65$ and $0 \leq K_a \leq 17$ have been analyzed together with data from two previous microwave and millimeter wave studies. The ground state rotational and **quartic** centrifugal distortion constants, their vibrational changes, and the sextic centrifugal distortion constants were used in a calculation of the **quartic** force field together with data from infrared studies.

1. INTRODUCTION

OC1O is an important stratospheric molecule which is particularly abundant during the polar nights (1, 2). It is thought to be formed in the bimolecular reaction



Thus, it is viewed as an indicator for the stratospheric bromine chemistry. Photolysis removes OC1O via



In the gas phase scheme 2 is by far the dominant one (3). Therefore, for almost each Br atom formed according to scheme 1 one O atom is released, rendering the gas phase formation and photolysis of OC1O essentially neutral towards ozone destruction. The quantum yield of scheme 3 is about 0.1 for OC1O dissolved in water (4); in this case OC1O contributes to net ozone loss. Isolated OC1O molecules in ice (5) or on ice surfaces (6) are photoisomerized to ClOO; its rapid decomposition into Cl + O₂ leads to O₃ loss. Oligomers of OC1O in this medium lead to ClClO₂ and possibly higher chlorine oxides (5, 6). Thus, the photochemistry of OC1O in or on ice is very similar to that in cryogenic rare gas matrices (7).

Currently its vibrationally structured spectrum in the near-UV (8) is used to determine the amount of atmospheric OC1O (2). With the increase in sensitivity of microwave limb sounding and similar techniques in recent years it may be possible to monitor OC1O employing millimeter and submillimeter spectroscopy.

OC1O has been known for almost two hundred years. It is one of few simple radicals that are

quite stable at room temperature. Curl *et al.* have analyzed its rotational spectrum for the two most abundant isotopomers, $0^{35}\text{Cl}10$ and $0^{37}\text{Cl}10$, in detail for the first time more than 35 years ago (9). Several additional investigations have been carried out in the microwave and millimeterwave regions, the most recent ones being the extensive studies by Tanoura *et al.* on the ground vibrational states (10) and by Miyazaki *et al.* on the (100), (01 0), (001), and (020) states (11).

The vibrational spectrum of OC1O has been investigated several times, most recently and most thoroughly by Ortigoso *et al.* They analyzed all three fundamental (12-14), the $2\nu_1$, and the $\nu_1 + \nu_3$ bands for both isotopomers (15), as well as the $\nu_1 + \nu_2 - \nu_2$ hot band and the weak $\Delta K_a = 2$ Fermi interaction between ν_1 and $2\nu_2$ (12). The most recent study OC1O isolated in rare gas matrices has been carried out by Müller and Winner. They obtained band positions for all three fundamentals and some overtones and combination bands for six isotopomers containing $^{35/37}\text{Cl}$ and $^{16/18}\text{O}$ (7).

In the course of the study of chlorine oxides of atmospheric interest extensive spectra of OC1O have been recorded at JPL in the millimeter and submillimeter regions. The analyses of these spectra are presented here mainly to improve the predictions of the OC1O submillimeter spectrum in the ground vibrational state and to derive a quartic force field.

II. EXPERIMENTAL

Details of the experimental setup are given in Ref. (16). Phase-locked klystrons were used as sources, in general in combination with an harmonic generator. In one set of experiments OC1O was obtained by passing Cl_2 over NaClO_2 . The entire spectral region between 415 and 436 GHz was

recorded at - 50°C and total pressures of -2.5 Pa. These spectra also contained lines from a higher harmonic (520 -526 GHz). Additional, selected measurements have been made between 130 and 425 GHz at -0.3 Pa and - 18°C or room temperature, employing the hydrolysis of FC10₂ or the decomposition of C1C10₂ as sources of OC1O (17).

III. Analysis and Fitting of the Spectra

OC1O is a slightly asymmetric, prolate top ($\kappa = -0.9260$ for 0^{35}C1O in the (000) state) with its dipole moment of 1.792 D (18) along the b-axis. Only rotational levels with $K_a + K_c$ even and odd are allowed for transitions within vibrational states with b_2 (states with odd quanta in ν_3) and a_1 symmetry (all other states), respectively, because of the C_{2v} symmetry of the molecule, its 2B_1 electronic ground state, and the zero spin of the ^{16}O nuclei. The rotational, electron spin, and nuclear spin angular momenta are coupled in the following way:

$$\mathbf{N} + \mathbf{S} = \mathbf{J}, \quad (4)$$

$$\mathbf{J} + \mathbf{I}_{Br} = \mathbf{F}. \quad (5)$$

The eight strongest lines of a rotational transition correspond to $\Delta F = \Delta J = \Delta N$. In general, the rotational selection rules are $|\Delta N| \leq 1$, $|\Delta K_a| = 1$, and ΔK_c odd. Because of the high sensitivity of the spectrometer system and the high gain chosen, some rotational transitions with $\Delta K_a = 3$ were assigned as well as some hyperfine or fine structure components having $\Delta F \neq \Delta N$ or $\Delta J \neq \Delta N$. On the other hand, some very strong lines overloaded the detector, and they were not used in the final fit.

Initial predictions were based on the data of Refs. (10) and (11). Several stronger features

were readily assignable based on their predicted positions, uncertainties, relative intensities, and fine and hyperfine patterns. These lines were included in the fits which resulted in improved predictions. Eventually very weak absorption became assignable. The range of quantum numbers N and K_u , the number of rotational transitions, and the number of fine and hyperfine components newly observed and used in the final fits is given in Table 1 for each isotopomer and each vibrational state. The complete lists of newly observed transitions have been deposited at ???; they are also available from one of the authors (HSPM). A machine-readable list of OC1O frequencies, intensities, and assignments in the ground vibrational state is available online in the JPL Submillimeter, Millimeter, and Microwave Line Catalog (<http://spec.jpl.nasa.gov>) (19).

The OC1O Hamiltonian can be written as

$$\mathcal{H} = \mathcal{H}_{\text{rot}} + \mathcal{H}_{\text{fs}} + \mathcal{H}_{\text{hfs}}, \quad (6)$$

where \mathcal{H}_{rot} is a Watson S reduction of the rotational Hamiltonian in the $1'$ representation which contains up to octic centrifugal distortion terms; \mathcal{H}_{fs} is a fine structure Hamiltonian describing the electron spin-rotation with quartic distortion terms; and \mathcal{H}_{hfs} is a hyperfine structure Hamiltonian which includes spin-spin, nuclear quadruple, and nuclear spin-rotation coupling. This Hamiltonian is similar to the one previously used (10,11); however, additional distortion and nuclear spin-rotation coupling terms were required to fit the present OC1O spectrum to within experimental uncertainties.

Predictions and fittings were done with Pickett's programs `SPCAT` and `SPFIT` (20). The 1σ uncertainties attributed to individual transitions were in general one twentieth of the half-width; they were increased for lines with low signal-to-noise ratio or incompletely resolved lines. Completely blended lines were fit as the intensity weighted average of their components. All parameters are positively defined, except for D_J , D_{JK} , and D_K .

The two isotopomers were fit together for each vibrational state. Each vibrational state was fit separately, except for the $V_2 = 1$ and 2 states, which were fit together. For the $v_i = 1$ state, ground state constants were kept fixed, and changes ΔC_i from the ground state constants C_0 were introduced as far as necessary. They were defined as

$$\Delta^1 C_i = C_i^1 - C_0, \quad (6)$$

where C_i^1 designates $v_i = 1$ spectroscopic constants. For the $V_2 = 2$ state changes from the ground state were in general assumed to be twice the value of those from the $v_2 = 1$ state. For some constants it was necessary to introduce second differences $\Delta^2 C_2$ which were defined as

$$\Delta^2 C_2 = C_2 - C_0 - 2 \Delta^1 C_2, \quad (7)$$

where C_2 designates $V_2 = 2$ spectroscopic constants. Some high order parameters were common to both isotopomers. The ratios of some hyperfine constants were fixed to the isotopic ratios determined for the Br nuclei in atomic beam experiments (21). For some of the highest order parameters, the present data justified using only a subset of the possible constants. In such cases, the choice of parameters may not be unique, but the effect *on the* lower order parameters and their interpretation is deemed to be insignificant. The final spectroscopic constants are given in Tables 2-7.

IV. FORCE FIELD CALCULATION

Enharmomic force field calculations have been made using a least-squares fitting program that is described in detail elsewhere (22). The input data were weighted inversely to the squares of their attributed uncertainties. The weights were adjusted so that all of the input data was reproduced

similarly well. The input data with their final attributed uncertainties in parentheses were the ground state rotational and **quartic** centrifugal distortion constants (100 times experimental uncertainties), the change in rotational and **quartic** centrifugal distortion constants for the first excited vibrational states (10 times experimental uncertainties, except for d 'A₁, where a factor of 30 was used), the ground state sextic distortion constants (30 times experimental uncertainties), the **wavenumbers** of the fundamental vibrations (12-14; 0.05 cm⁻¹ uncertainties), and the **anharmonic** constants x_{11} , x_{12} (for 0³⁵C10 only), x_{13} (15), x_{33} (7; all with 0.05 cm⁻¹ uncertainties), and for 0³⁵C10 only x_{22} and x_{23} (23; 0.15 cm⁻¹ uncertainties). The value for x_{33} is from a matrix study. Its gas phase value was estimated by scaling the matrix value with the ratio of gas phase and matrix values for ν_3 . The resulting force field is given in Table 9 under heading a.

This force field had rather large residuals for some of the fundamentals, **anharmonic** constants, the centrifugal distortion constants, and their vibrational changes, particularly D_K , H_K , and A^1D_K . It was suspected that the large residuals to some extent were caused by the approximations made: the (negative) changes in the vibrational and **quartic** distortion constants were taken for the α 's and β 's, respectively, and the ground state sextic distortion constants were taken for their equilibrium values. However, the vibrational dependence of the rotational constants is (24)

$$B_{\nu}^g = B_e^g - \sum \alpha_i^g (\nu_i + 1/2) + \sum \gamma_{ij}^g (\nu_i + 1/2)(\nu_j + 1/2) + \dots, \quad (8)$$

where the vibrational state ν is specified by the quantum numbers ν_i , ν_j , B_e^g is the equilibrium rotational constant, and α_i^g , γ_{ij}^g , . . . are the vibration rotation interaction constants for the g-axis.

Thus

$$B_e^g = B_0^g + 1/2 \sum \alpha_i^g - 1/4 \sum \gamma_{ij}^g + \dots, \quad (9)$$

$$\Delta^1 B_{\nu_i}^g = \alpha_i^g - 2 \gamma_{ii}^g - 1/2 \sum_{j \neq i} \gamma_{ij}^g + \dots, \quad (10)$$

$$\Delta^2 B^g_i = 2\gamma^g_{ii} + \dots \quad (11)$$

etc. Analogous relationships hold for the D 's and H 's. Since the respective higher order contributions due to the bending coordinate are known quite well and since for many constants these appear to be the largest higher order contributions, the following constants were defined:

$$H' = HO - A^1 H_2/2, \quad (12)$$

$$\Delta^1 B^g_2' = A^1 B^g_2 - \Delta^2 B^g_2, \quad (13)$$

and
$$A^1 D_2' = A^1 D_2 - \Delta^2 D_2. \quad (14)$$

The H' , $A^1 B^g_2'$, and $A^1 D_2'$ were used in the fit instead of H , $A^1 B^g_2$, and $A^1 D_2$, respectively. The resulting force field is presented in Table 9 under heading b. Because it had much smaller residuals than the one described above, it is the preferred force field. Higher order corrections other than the ones used for the second force field calculation have been neglected because they are known only in few instances. Also included in Table 9 are two experimental force fields with up to cubic and quadratic force constants, respectively, and an *ab initio* force field (25) for comparison purpose. The input data for the preferred force field and the residuals are presented in Tables 10 and 11.

V. DISCUSSION

The spectroscopic parameters of the ground vibrational state of OC1O have been improved for both isotopomers. A complete set of sextic as well as some octic distortion constants have been determined for the first time. Therefore, strong and moderately strong lines can be predicted precisely well into the submillimeter region. In addition, a complete set of quartic spin-distortion terms

and nuclear spin-rotation constants are available. The spin-distortion terms in the S reduction (26) are quite different from those in the A reduction. Very recently it became possible to use the A reduced spin-distortion constants in the SPFIT and SPCAT (20) programs. In order to allow a better comparison with the previously reported values (13), an A reduced Hamiltonian has been used for the ground state of OC1O. The S and A reduced quartic spin-distortion constants of $^{16}\text{O}^{18}\text{O}$ are given in Table 12 together with values from Ref. (13) and data for $^{16}\text{O}^{17}\text{O}$ (27). The previous OC1O values (13) for δ_N^S and δ_K^S agree quite well with the present, more precise ones. The agreement is reasonable for Δ_{NK}^S and Δ_K^S if one takes into consideration that in Ref. (13) Δ_{KN}^S was fixed to $-\Delta_{NK}^S$ and Δ_N^S was not determined. The spin-distortion terms of OBrO in the A reduction are also quite different from those in the S reduction. The OBrO values are all larger than the OC1O values in the A reduction, as is the case for the electron spin-rotation constants (27), while the relationships are more complex in the S reduction. A common set of spin-distortion terms for both isotopomers is less justified in the A reduction than in the S reduction because several of the constants are much larger in magnitude but have similar uncertainties.

Brown and Sears (26) have discussed a relationship between the quartic spin-distortion terms η_{iiii} , derived from the determinable D^S constants, and the mechanical distortion terms τ_{iiii} . For an orthorhombic molecule this relationship is

$$\eta_{iiii} = \tau_{iiii}\epsilon_i/2B_i. \quad (15)$$

As is shown in Table 13, the agreement is rather poor for both OC1O and OBrO. In each case the sign is opposite, and only the ordering in magnitude agrees. Brown and Sears have done similar calculations for NH_2 (26); the calculated values for η_{aaaa} and η_{bbbb} were smaller than the experimental ones by a factor of -2 and -1.5, respectively. Part of these deviations may be explained by the large

changes of the spin-distortion constants upon excitation of different vibrational states, which are given in Table 4 for OC1O. OBrO (27) and other radicals exhibit similarly large changes.

It has been possible to determine nuclear spin-rotation coupling constants for the first time. Endo *et al.* have proposed a relationship between the electronic and nuclear spin-rotation coupling constants (28):

$$|C_{gg}/\epsilon_{gg}| = |a/A_{so}|, \quad (16)$$

with $A_{so} = 365 \text{ cm}^{-1}$, the average of $A_{so}(\text{Cl})$ and $A_{so}(\text{O})$ weighted according to the spin-density (-48% on the Cl atom) which were determined from the spin-spin coupling constants (29, 30), and $a = 2\beta g_N \beta_N \langle 0|r^{-3}|n \rangle = 439 \text{ MHz}$ approximated by $5/4T_{aa} = 201 \text{ MHz}$. The experimental values for ^{35}ClO and those calculated from Eq. 16 are compared in Table 14. The calculated values of C_{aa} and C_{bb} are too small by a factor of -2, and that of C_{cc} is too small by a factor of -70.

In Table 15 $A''_{ii} = C_{ii}/B_i$ of ^{35}ClO are compared with those of O^{79}BrO . Their ratios are expected to be close to $g_{\text{Cl}}\langle r_{\text{Cl}}^{-3} \rangle / g_{\text{Br}}\langle r_{\text{Br}}^{-3} \rangle$, where g_X is the nuclear g-value of the nucleus X (31). The ratios of the A''_{ii} are slightly smaller, as is the case for ClF and BrF.

The spectroscopic constants for the $V_2 = 1$ and 2 states have been improved somewhat, of course with the exception of the ν_2 band origins; to our knowledge no rovibrational transitions of the 2 V_2 band have been reported yet. The signal-to-noise ratio in a neon matrix spectra of OC1O around 900 cm^{-1} enables the estimation of an upper limit for the 2 V_2 band as - 1/2000 of the V_3 intensity (7, 3.5). The data for the $\nu_1 = 1$ and $V_3 = 1$ states are included more for completeness reason and in order to obtain a uniform set of input data for the force field calculation. Inspection of the $V_1 = 1$ and $\nu_2 = 2$ energy levels and data on the $\Delta K_a = 2$ Fermi resonance between these states (12) indicate that the lines reported in this study are not significantly affected by the $\Delta K_a = 2$ interaction

constant used in Ref. (12) to account for the Fermi resonance. However, the lines observed for these states in the present study may be helpful for a future detailed analysis of the resonance.

As far as comparisons are possible, the agreement among the constants of the preferred anharmonic force field and the experimental and *ab initio* constants in Table 8 is good, particularly for the larger ones. Most of the input data is reproduced well by the preferred force field. To our knowledge, the vibrational changes in the quartic distortion constants have not been used as input data. They have been reproduced reasonable well if one considers that they are strongly affected by small changes in the force constants and that some of these changes are quite small. The residual for x_{23} is rather large, -2.64 cm^{-1} . It is noteworthy that the value from the preferred force field, -5.04 cm^{-1} is quite close to -5.5 cm^{-1} from high level *ab initio* calculations (25). Since the experimental value for x_{23} is from a low resolution study (23) it is conceivable that this value is in error by a few wavenumbers. The residual for X_{22} is also quite large, -1.04 cm^{-1} , but the experimental value of -3.99 cm^{-1} from a high resolution study (12) is in very good agreement with *ab initio* values of -4.1 cm^{-1} (25). The values for X_{22} from the preferred empirical force field, -0.42 cm^{-1} , and from the *ab initio* calculations, -0.35 cm^{-1} , are closer to -0.15 cm^{-1} from Ref. (23) than to $0.4 \pm 0.1 \text{ cm}^{-1}$ from Ref. (15). Since these differences are comparatively small, the comparison should be taken with a grain of salt.

For a planar molecule the inertial defects Δ_v and their differences $\Delta \Delta_v$ can be calculated from the harmonic part of the force field. A comparison of the calculated values $\Delta \Delta_v$ with the experimental ones is given in Table 16. The agreement is quite good, and the small deviations are very similar in magnitude and of the same sign for all three fundamentals and both isotopomers. This can be taken as a piece of evidence that the rotational constants in the (1 00) and (020) states are only

slightly effected by the Fermi resonance.

ACKNOWLEDGMENTS

We would like to thank Dr. Kirk Peterson for communicating *ab initio* results prior to publication and Dr. K. Tanaka for making available the excited state microwave line positions. H. S. P. M. and M. B. thank the National Research Council for NASA-NRC Resident Research Associateships. Part of the research was performed at the Jet Propulsion Laboratory, California Institute of Technology, under a contract with the National Aeronautics and Space Administration.

REFERENCES

1. R. P. Wayne, G. Poulet, P. Biggs, J. P. Burrows, R. A. Cox, P. J. Crutzen, G. D. Hayman, M. E. Jenkin, G. Le Bras, G. K. Moortgat, U. Platt, and R. N. Schindler, *Atmos. Envir.* **29**, 2677-2881 (1995).
2. (a) K. Kreher, J. G. Keys, P. V. Johnston, U. Platt, and X. Liu, *Geophys. Res. Lett.* **23**, 1545-1548 (1996); (b) M. Gil, O. Puertedura, M. Yela, C. Parrendo, D. B. Jadhav, and B. Thorkelsson, *ibid.* 3337-3340; (c) M. Y. Danilin, N.-D. Sze, M. K. W. Ko, J. M. Rodriguez, and M. Prather, *ibid.* 153-156.
3. A. Furlan, H. A. Scheld, J. R. Huber, *J. Chem. Phys.* **106**, 6538-6547 (1997); and references therein.
4. J. Thøgersen, P. U. Jepsen, C. L. Thomsen, J. Aa. Poulsen, J. R. Byberg, and S. R. Keiding, *J. Phys. Chem. A* **101**, 3317-3323 (1997); and references therein.
5. C. J. Pursell, J. Conyers, and C. Denisen, *J. Phys. Chem.* **100**, 15450-15453 (1996).
6. J. D. Graham, J. T. Roberts, L. D. Anderson, and V. H. Grassian, *J. Phys. Chem.* **100**, 19551-19558 (1996).
7. H. S. P. Müller and H. Winner, *J. Phys. Chem.* **97**, 10589-10598 (1993).
8. (a) A. Wahner, G. S. Tyndall, and A. R. Ravishankara, *J. Phys. Chem.* **91**, 2734-2738 (1987); (b) E. C. Richard and V. Vaida, *J. Chem. Phys.* **94**, 153-162 (1991).
9. R. F. Curl, Jr., J. L. Kinsey, J. G. Baker, J. C. Baird, G. R. Bird, R. F. Heidelberg, T. M. Sugden, D. R. Jenkins, and C. N. Kenney, *Phys. Rev.* **121**, 1119-1123 (1961).
10. M. Tanoura, K. Chiba, K. Tanaka, and T. Tanaka, *J. Mol. Spectrosc.* **95**, 157-181 (1982).

11. K. Myazaki, M. Tanoura, K. Tanaka, and T. Tanaka, *J. Mol. Spectrosc.* **116**,435-449 (1986).
12. J. Ortigoso, R. Escribano, J. B. Burkholder, C. J. Howard, and W. J. Lafferty, *J. Mol. Spectrosc.* **148**,346-370 (1991).
13. J. Ortigoso, R. Escribano, J. B. Burkholder, and W. J. Lafferty, *J. Mol. Spectrosc.* **155**,25-43 (1992).
14. J. Ortigoso, R. Escribano, J. B. Burkholder, and W. J. Lafferty, *J. Mol. Spectrosc.* **156**,89-97 (1992).
15. J. Ortigoso, R. Escribano, J. B. Burkholder, and W. J. Lafferty, *J. Mol. Spectrosc.* **158**, 347-356 (1993).
16. R. R. Friedl, M. Birk, J. J. Oh, and E. A. Cohen, *J. Mol. Spectrosc.* **170**,383-396 (1995).
17. H. S. P. Müller and E. A. Cohen, *J. Phys. Chem. A* **101**,3049-3051 (1997).
18. K. Tanaka, and T. Tanaka, *J. Mol. Spectrosc.* **98**,425-452 (1983).
19. (a) R. L. Poynter and H. M. Pickett, *Appl. Opt.* **24**,2235-2240 (1985); (b) H. M. Pickett, R. L. Poynter, E. A. Cohen, M. L. Delitsky, J. C. Pearson, and H. S. P. Müller, "Submillimeter, Millimeter, and Microwave Line Catalog," JPL Publication 80-23, Revision 4, Pasadena, CA, 1996.
20. H. M. Pickett, *J. Mol. Spectrosc.* **148**,371-377 (1991).
21. H. H. Brown and J. G. King, *Phys. Rev.* **142**,53-59 (1966).
22. G. O. Sørensen, to be published.
23. A. W. Richardson, R. W. Redding, and J. C. D. Brand, *J. Mol. Spectrosc.* **29**,93-108 (1969).
24. E. g., W. Gordy and R. L. Cook, "Microwave Molecular Spectra," 3rd cd., Wiley, New York,

- 1984.
25. K. A. Peterson, to be published.
 26. J. M. Brown and T. J. Sears, *J. Mol. Spectrosc.* 75, 111-133 (1979).
 27. H. S. P. Müller, E. E. Miller, and E. A. Cohen, submitted to *J. Chem. Phys.*
 28. Y. Endo, S. Saito, and E. Hirota, *J. Mol. Spectrosc.* 97, 204-212 (1983).
 29. R. N. Dixon and H. W. Kroto, *Trans. Faraday Soc.* 59, 1484-1489 (1963).
 30. E. g., E. Hirota, "High-Resolution Spectroscopy of Transient Molecules," Springer, Berlin, 1985.
 31. E. g., J. S. Muentzer, in "Molecular Structure and Properties," (A. D. Buckingham, Ed.), MTP International Review of Science, Physical Chemistry, Series II, Vol. 2, Butterworths, London, 1975).
 32. J. R. Morton, and K. F. Preston, *J. Magn. Reson.* 30, 577-583 (1978).
 33. (a) B. Fabricant and J. S. Muentzer, *J. Chem. Phys.* 66, 5274-5277 (1977); (b) R. E. Willis, Jr., and W. W. Clark III, *J. Chem. Phys.* 72, 4946-4950 (1980).
 34. H. S. P. Müller and M. C. L. Gerry, *J. Chem. Phys.* 103, 577-583 (1995).
 35. H. S. P. Müller and H. Winner, unpublished.

Table Captions

TABLE 1: Number of Newly Observed Rotational Transitions, Fine Structure and Hyperfine Structure Components, and Range of Quantum Numbers Used in the Final Fits of OC10.

TABLE 2: Rotational and Centrifugal Distortion Constants' C (MHz) of 0^{35}C10 in the Ground Vibrational State,^b Their Changes A^1C_i in the First Excited States, and Their Second Differences A^*C_2 for the $v_2 = 2$ State,^b

TABLE 3: Rotational and Centrifugal Distortion Constants^a C (MHz) of 0^{37}C10 in the Ground Vibrational State, Their Changes A^1C_i in the First Excited States,^b and Their Second Differences A^*C_2 for the $V_2 = 2$ State.^b

TABLE 4: Electron Spin-Rotation Coupling Constants and Quartic Distortion Terms' C (MHz) of 0^{35}C10 in the Ground Vibrational State, Their Changes A^1C_i in the First Excited States,^b and Their Second Differences Δ^2C_2 for the $V_2 = 2$ State.^b

TABLE 5: Electron Spin-Rotation Coupling Constants' C (MHz) of 0^{37}C10 in the Ground Vibrational State, Their Changes A^1C_i in the First Excited States,^b and Their Second Differences Δ^2C_2 for the $V_2 = 2$ State.^b

TABLE 6: Spin-Spin, Nuclear Quadruple, and Nuclear Spin-Rotation Coupling Constants^a C (MHz) of 0^{35}C10 in the Ground Vibrational State and Their Changes A^1C_i in the First Excited States.^b

TABLE 7: Spin-Spin, Nuclear Quadruple, and Nuclear Spin-Rotation Coupling Constants' C (MHz) of 0^{37}C10 in the Ground Vibrational State and Their Changes A^1C_i in the First Excited States.^b

TABLE 8: Experimental and *ab initio* Structural Parameters (pm, Degrees) and Force

Constants ($\text{aJ } \text{\AA}^{-n}$) of OC1O.

TABLE 9: Fundamental Vibrations (cm^{-1}), the Rotational^a(MHz) and Quartic Centrifugal Distortion Constants^a(kHz) of $^{35}\text{C1O}$ Used for the Force Field Calculation and Residuals C-oh.

TABLE 10: Fundamental Vibrations (cm^{-1}), the Rotational^a(MHz) and Quartic Centrifugal Distortion Constants^a(kHz) of $^{37}\text{C1O}$ Used for the Force Field Calculation and Residuals C-oh.

TABLE 11: Enharmonic Constants (cm^{-1}) and Sextic Centrifugal Distortion Constants^a(Hz) of OC1O Used for the Force Field Calculation and Residuals c- o^b.

TABLE 12: Comparison of Electron Spin-Rotation Coupling Constants of $^{35}\text{C1O}$ and ^{79}BrO in the A and S Reduction.

TABLE 13: Comparison of Experimental and Calculated^aDiagonal Quartic Spin-Distortion Terms η_{iiii} (kHz) of OC1O and OBrO.

TABLE 14: Compassion of Experimental Nuclear Spin-Rotation Coupling Constants of $^{35}\text{C1O}$ with Those Calculated From the Electron Spin-Rotation Coupling Constants' (kHz).

TABLE 15: Comparison of Reduced Nuclear Spin-Rotation Coupling Constants^a $A''_{ii} \cdot 10^6$ of $^{35}\text{C1O}$ and ^{79}BrO .

TABLE 16: Comparison of Inertial Defect Differences Δ_v^a ($\text{amu } \text{\AA}^2$) of OC1O with Those Calculated from the Harmonic Part of the Force Field.

	ground state		V, ₁		v ₂ = 1		v ₃ = 1		v ₂ = 2	
	O ³⁵ ClO	O ³⁷ ClO	O ³⁵ ClO	O ³⁷ ClO	O ³⁵ ClO	O ³⁷ ClO	O ³⁵ ClO	O ³⁷ ClO	O ³⁵ ClO	O ³⁷ ClO
N _{rot}	43	41	9	8	18	16	9	2	8	5
N _{fs}	70	66	15	13	31	28	15	3	15	8
N _{hfs}	243	233	46	37	110	103	47	9	39	17
N _{min} - N _{max}	2-65	6-60	8-33	8-33	5-51	6-45	6-36	24-31	5-35	11-45
K _{min} - K _{max}	0-17	0-15	0-6	0-6	0-13	0-10	0-6	0-4	0-7	0-6

C	(000)	(100)	(010)	(001)	(020)
<i>A</i>	52081.25077 (187)	-53.9267 (39)	998.16921 (273)	-481.6565 (55)	40.3241 (70)
<i>B</i>	9952.60526 (40)	-60.02369 (69)	-9.13811 (52)	-54.58752 (109)	-0.20859 (139)
<i>C</i>	8334.21980 (35)	-53.46729 (68)	-24.03922 (51)	-42.869 98(1 12)	-0.10705 (132)
$D_N \cdot 10^3$	8.517213 (300)	-0.04974 (95)	-0.04324 (68)	0.14379 (95)	0.00012 (149)
$D_{NK} \cdot 10^3$	-112.6414 (50)	7.3346 (81)	-4.8161 (63)	-9.7959 (149)	-0.3102 (74)
$D_K \cdot 10^3$	2051.8552 (268)	22.498 (174)	222.721 (59)	-2.618 (131)	32.279 (101)
$d_1 \cdot 10^3$	-2.304527 (43)	0.003067 (200)	-0.008266 (161)	-0.02832 (50)	-0.000015 (92)
$d_2 \cdot 10^3$	-0.1387765 (257)	-0.018994 (140)	-0.025431 (75)	0.01369 (26)	-0.001034 (58)
$H_N \cdot 10^6$	0.012731 (52)		-0.000475 (226)		
$H_{NK} \cdot 10^6$	-0.29579 (189)		0.00031 (356)		
$H_{KN} \cdot 10^6$	-18.556 (40)		-2.986 (100)		
$H_K \cdot 10^6$	272.23 (32)		61.67 (61)		
$h_1 \cdot 10^6$	0.0072136 (175)		0.000301 (132)		
$h_2 \cdot 10^6$	0.0009478 (168)		-0.000062 (94)		
$h_3 \cdot 10^6$	0.0004943 (51)		0.0001505 (245)		
$L_{NK} \cdot 10^9$	-0.1005 (165)				
$L_{KKN} \cdot 10^9$	4.611 (166)				
$L_K \cdot 10^9$	-51.40 (123)				

^aNumbers in parentheses are one standard deviation in units of least significant figures.

^bSee text.

c	(000)	(100)	(010)	(001)	(020)
<i>A</i>	50736.86492 (195)	-63.2448 (71)	971.02017 (312)	-458.4618 (139)	38.9003 (92)
<i>B</i>	9953.12310 (33)	-59.43640 (107)	-9.16501 (54)	-54.07793 (275)	-0.20703 (157)
<i>c</i>	8299.13659 (30)	-52.48873 (98)	-24.07208 (54)	-42.27209 (280)	-0.10490(150)
$D_N \cdot 10^3$	8.459061 (291)	°	°	0.14347 (261)	°
$D_{NK} \cdot 10^3$	-108.1277 (44)	7.4396 (132)	-4.6068 (67)	-9.4724 (359)	°
$D_K \cdot 10^3$	1947.2686 (358)	18.867 (287)	210.382 (95)	°	30.711 (194)
$d_1 \cdot 10^3$	-2.329154 (68)	°	-0.007934 (168)	-0.02810 (31)	°
$d_2 \cdot 10^3$	-0.1425382 (389)	-0.019147 (153)	-0.025848 (76)	0.01653 (43)	°
$H_N \cdot 10^6$	0.012744 (60)		°		
$H_{NK} \cdot 10^6$	-0.30286 (199)		°		
$H_{KN} \cdot 10^6$	-17.439 (39)		°		
$H_K \cdot 10^6$	252.18 (34)		47.61 (73)		
$h_1 \cdot 10^6$	0.0072136 (330)		°		
$h_2 \cdot 10^6$	0.0010060 (260)		°		
$h_3 \cdot 10^6$	0.0004971 (64)		°		
$L_{NK} \cdot 10^9$	°				
$L_{KKN} \cdot 10^9$	°				
$L_K \cdot 10^9$	-48.63 (122)				

^{a,b} See footnotes Table 2.

° Common constants for both isotopomers.

c	(000)	(loo)	(010)	(001)	(020)
ϵ_{aa}	-1388.2848 (126)	-9.357 (46)	12.8171 (220)	-26.077 (52)	3.583 (50)
ϵ_{bb}	-216.9315 (58)	-3.9101 (143)	-0.3789 (87)	-2.8246 (166)	-0.0224 (178)
ϵ_{cc}	4.6003 (54)	0.1493 (141)	0.0489 (82)	0.1442 (191)	0.0091 (169)
$D_N^S \cdot 10^3$	-0.1210 (58)				
$D_{NK}^S \cdot 10^3$	-1.508 (115)				
$D_{KN}^S \cdot 10^3$	-3.457 (140)				
$D_K^S \cdot 10^3$	-0.702 (151)	-4.16 (201)	-10.895 (267)	2.40 (177)	
$d_1^S \cdot 10^3$	-0.09365 (67)	0.0316 (98)	0.00216 (95)	0.0249 (95)	
82''103	-0.02277 (37)	-0.0109 (62)	0.00255 (74)		

^{a, b} See footnotes Table 2.

c	(000)	(100)	(010)	(001)	(020)
ϵ_{aa}	-1352.4662 (180)	-9.303 (98)	12.5907 (220)	-25.014 (71)	3.504 (50)
ϵ_{bb}	-216.9396 (73)	-3.7746 (337)	-0.3545 (86)	-2.7380 (255)	^c
ϵ_{cc}	4.5366 (69)	0.2106 (333)	0.0887 (82)	0.1831 (257)	^c

^a Common spin-distortion terms were used for both isotopomers. See also footnote Table 2.

^b See text.

^c Common constants for both isotopomers.

c	(000)	(100)	(010)	(001)
a_F	46.1451 (129)	-0.067 (68) ^c	0.0833 (88) ^c	-0.507 (43) ^c
T_{aa}	-77.6899 (168)	0.575 (75) ^c	0.0724 (121) ^c	0.684 (61) ^c
$T.^d$	-243.9167 (247)	2.013 (42) ^c	0.2374 (141) ^c	2.347 (52) ^c
χ_{aa}	-51.831 (45)	0.217 (168) ^c	-0.013 (45) ^c	-0.161 (158) ^c
$\chi.^e$	-46.547 (54)	-0.495 (99) ^c	-0.105 (35) ^c	-0.744 (131) ^c
$C_{aa} \cdot 10^3$	44.07 (334) ^c			
$C_{bb} \cdot 10^3$	7.84 (107) ^c			
$C_{cc} \cdot 10^3$	6.99 (97) ^c			

^{a, b} See footnotes Table 2.

^c Isotopic ratio fixed, see Table 7.

^d $T. = T_{bb} - T_{cc}$.

^e $\chi. = \chi_{bb} + \chi_{cc}$.

c	(000)	(100)	(010)	(001)
a_F	38.4071 (226)	-0.056 (56) ^c	0.0693 (73) ^c	-0.422 (35) ^c
T_{aa}	-64.6999 (271)	0.478 (62) ^c	0.0603 (101) ^c	0.570 (51) ^c
$T.^d$	203.0706 (273)	1.676 (35) ^c	0.1976 (117) ^c	1.954 (43) ^c
χ_{aa}	-40.902 (91)	0.171 (132) ^c	-0.010 (36) ^c	-0.127 (124) ^c
χ^{-e}	-36.507 (61)	-0.390 (78) ^c	-0.083 (27) ^c	-0.586 (104) ^c
$C_{aa} \cdot 10^3$	35.73 (271) ^c			
$C_{bb} \cdot 10^3$	6.52 (89) ^c			
$C_{rr} \cdot 10^3$	5.82 (80) ^c			

^{a,b} See footnotes Table 2. ^c Isotopic ratio fixed, see Table 6. ^{d,e} See footnotes Table 6.

	experimental				<i>ab initio</i> ^c
	a	b	c	d	
r	146.9873 (22)	146.98236 (120)	146.9839		147.187
α	117.3969 (18)	117.40664 (100)	117.4033		117.655
f_{rr}	7.0435 (150)	7.0342 (89)	7.055	7.024	6.981
$f_{rr'}$	-0.1309(130)	-0.2101 (78)	-0.193	-0,188	-0.204
f_{ra}	0.0208 (75)	-0.0276 (43)	0.018	-0,005	-0.014
f_{aa}	1.3727 (44)	1.3982 (28)	1.382	1.398	1.417
f_{rrr}	-52.314 (220)	-51.806 (130)	-52,035		-51.141
$f_{rrr'}$	0.041 (45)	0.227 (25)	0.040		-0.217
f_{rra}	-0.246 (66)	0,094 (37)	-0.335		-0.062
$f_{rr'a}$	-0.156 (17)	-0.2071 (96)	-0.265		-0.125
f_{raa}	-1.8519 (220)	-1.8864 (120)	-2.003		-1.908
f_{aaa}	-2.0409 (180)	-1.9054 (120)	-1.885		-2.088
f_{rrrr}	319.3 (220)	300.4 (150)			300.951
$f_{rrrr'}$	-27.1 (92)	-4.0 (60)			0.228
$f_{rrr'r'}$	6.9 (90)	10.3 (80)			8.455
f_{rrra}	10.5 (170)	1.6(110)			1.908
$f_{rrr'a}$	1.308	4.5 (34)			1.274
f_{rraa}	11.1 (31)	3.50 (200)			1.232
$f_{rr'aa}$	-0.9 (29)	3.18 (210)			3.761
f_{raaa}	4.480	2.98 (86)			4.441
f_{aaaa}	3.33 (100)	5.23 (1 10)			5.946

^aThis work.

^bThis work; preferred force field, see text.

^cRef. (11).

^dNe matrix data, Ref. (7); structure from Ref. (11).

^eMRCI+Q/ext-cc-pVQZ, Ref (25).

	(000)		(100)		(010)		(001)	
	ohs.	c-o	ohs.	c-o	ohs.	c-o	ohs.	c-o
ν_i			945.592	0.018	447.702	-0.186	1110.106	0.007
A	52081.251	-0.115	-53.927	-0.863	957.845	-0.139	-481.657	-2.335
B	9952.605	-0.260	-60.024	-0.072	-8.930	-0.004	-54.588	-0.266
C	8334.220	0.281	-53.467	0.085	-23.932	0.019	-42.870	0.397
D_N	8.5172	0.0451	-0.0497	-0.0235	-0.0435	0.0011	0.1438	-0.0491
D_{NK}	-112.614	-0.307	7.335	2.112	-4.506	0.884	-9.796	4.098
D_K	2051.86	-9.76	22.498	4.349	190.442	4.123	-2.618	-11.336
d_1	-2.3045	-0.0055	0.0031	0.0210	-0.0083	0.0005	-0.0283	0.0173
d_2	-0.1388	0.0038	-0.0189	0.0130	-0.0244	0.0090	0.0137	-0.0071

^a Changes from the ground vibrational state, A^1C , were used for the excited states. Values for (010) were corrected for the second changes, A^2C , see text.

^b Value calculated from the force field minus input value.

	(000)		(100)		(010)		(001)	
	obs.	c-o	obs.	c-o	obs.	c-o	obs.	c-o
v_i			936.602	-0.015	444.824	-0.168	1098.247	0.000
A	50736.865	-0.384	-63.245	-0.699	932.120	-0.065	-458.462	-2.379
B	9953.123	-0.243	-59.436	-0.055	-8.958	-0.017	-54.078	-0.270
c	8299.137	0.294	-52.489	0.101	-23.967	0.010	-42.272	0.363
D_N	8.4591	0.0448	-0.0497	-0.0234	-0.0434	0.0016	0.1435	-0.0508
D_{NK}	-108.128	-0.296	7.440	2.162	-4.297	0.844	-9.472	3.793
D_K	1947.27	-9.18	18.87	4.64	179.67	4.14	-2.62	-9.46
$d,$	-2.3292	-0.0058	0.0031	0.0212	-0.0079	0.0006	-0.0281	0.0171
$d,$	-0.1425	0.0039	-0.0191	0.0127	-0.0248	0.0093	0.0130	-0.00903

^{a, b} See footnotes Table 9.

	0^{35}C10		0^{37}C10	
	ohs.	c-o	ohs.	c-o
x_{11}	-4.335	-0.262	-4.270	-0.241
x_{12}	-3.993	1.044		-2.901
x_{13}	-16.765	-0.011	-16.555	-0.029
x_{22}	-0.15	-0.266		-0.419
x_{23}	-2.4	-2.643		-4.932
x_{33}	-5.61	-0.038	-5.47	-0.028
H_N	0.01297	0.00033	0.01298	0.00028
H_{NK}	-0.2959	0.0076	-0.3030	0.0073
H_{KN}	-17.063	-0.193	-15.946	-0.200
H_K	241.40	-0.04	223.37	-0.00
$h_1 \cdot 10^3$	7.063	0.397	7.021	0.433
$h_2 \cdot 10^3$	0.979	0.065	1.037	0.013
$h_3 \cdot 10^3$	0.419	0.003	0.422	0.021

^{a, b} See footnotes Table 9.

	0^{35}C10			0^{79}BrO	
	S red. ^a	A red. ^c	A red. ^b	S red. [']	A red. ^a
D_N^S / Δ_N^S	-0.1210	-0.1614	-	-0.3725	-0.5962
D_{NK}^S / Δ_{NK}^S	-1.51	-18.89	-42.9	-0.625	-29.62
D_{KN}^S / Δ_{KN}^S	-3.46	15.40	^d	-0.305	34.03
D_K^S / Δ_K^S	-0.70	-2.04	-8.2	-17.21	-22.26
$d_1^S \text{ I } \delta_N^S$	-0.09365	-0.09396	-0.0843	-0.3433	-0.3433
$d_2^S \text{ I } \delta_K^S$	-0.02277	-7.499	-7.96	-0.1151	-11.756

^aThis work.

^bRef. 27.

^cRef. 13.

^d $\Delta_{KN}^S = -\Delta_{NK}^S$ set in the fit.

	0^{35}C10		0^{81}BrO	
	obs. ^b	talc. ^b	obs. ^c	talc. ^b
η_{aaaa}	-5.79	97.9	-18.51	106.0
η_{bbbb}	-0.354	0.586	-1.289	1.748
$\eta_{....}$	0.0208	-0.0046	0.0839	-0.0360

^a See text. ^b This work, ^c Derived from Ref. (27).

	exptl.	talc.
C_{aa}	44.1	25.5
C_{bb}	7.8	4.0
C_{cc}	7.0	0.1

^a See Eq. 16.

i	O ³⁵ ClO ^b	O ⁷⁹ BrO ^c	$\Lambda^n_{ii}(\text{Cl})/\Lambda^n_{ii}(\text{Br})$	$g_{\text{Cl}}\langle r_{\text{Cl}}^{-3}\rangle/g_{\text{Br}}\langle r_{\text{Br}}^{-3}\rangle^{\text{d}}$
a	0.85	5.72	0.149	0.215
b	0.79	5.06	0.156	0.215
c	0.84	5.00	0.168	0.215
<hr/>				
	³⁵ ClF ^e	⁷⁹ BrF ^f	$\Lambda^n_{ii}(\text{Cl})/\Lambda^n_{ii}(\text{Br})$	$g_{\text{Cl}}\langle r_{\text{Cl}}^{-3}\rangle/g_{\text{Br}}\langle r_{\text{Br}}^{-3}\rangle^{\text{d}}$
	1.40	8.38	0.167	0.215

^a $A_{ii} = C_{ii}/B_i$. ^b This work. ^c Ref. (27). ^d Refs. (24, 32).

^e Ref. (33). ^f Ref. (34).

	O^{35}ClO		O^{37}ClO	
	obs.	calc.	obs.	calc.
$\Delta A_{(100)}$	0.0734	0.0697	0.0701	0.0665
$\Delta A_{(010)}$	0.3112	0.3062	0.3174	0.3124
$\Delta A_{(001)}$	-0.0565	-0.0626	-0.0571	-0.0619
$\Delta A_{(020)}$	0.6233	0.6124	0.6356	0.6248

$$^a \Delta A_v = A_v - A_{(000)}$$